Fish and Shellfish Immunology 84 (2019) 1018–1029

Contents lists available at ScienceDirect

Fish and Shellfish Immunology

journal homepage: www.elsevier.com/locate/fsi

Full length article

Production and Function of Different Regions from Mytichitin-1 of *Mytilus coruscus*

Hong-han Liu, Mei-hua Fan, Hui-hui Liu, Peng-zhi Qi, Liao Zhi*

Key Laboratory for Marine Living Resources and Molecular Engineering, College of Marine Science, Zhejiang Ocean University, Zhoushan, 316022, PR China

ARTICLE INFO

Keywords:
Mytilus coruscus
Chitinase
Mytichitin-1
Antimicrobial peptide
Chitin-binding domain
Catalytic domain

ABSTRACT

Chitinase is an important enzyme for many physiological processes. Mytichitin-1 is a chitinase-like protein in *Mytilus coruscus*, and its C-terminal 55-AA fragment (mytichitin-CB) is a novel antimicrobial peptide, suggesting a new immune process in which chitinase is involved; mytichtin-1 may have various forms in the different biological processes of *M. coruscus*. Thus, the study of mytichitin-1 will be helpful for understanding the mechanism of mussel immune biology and the functional diversity of chitinase. In this study, mytichitin-1 was recombinantly expressed with different lengths, full-length mytichtin-1 (rMchi-F) and the N-terminal region (rMchi-N) in *Escherichia coli* BL21 with codon optimization. The results of SDS-PAGE, Western blotting, and mass spectrometry confirmed that the two forms of mytichitin-1 had been successfully recombinant expressed with a yield of 40 mg purified enzyme per L culture. In addition, the 55-AA fragment of mytichitin-CB was chemically synthesized (sMchi-CB). After purification and oxidation, the functions of the three protein products were analysed, including chitin degradation, chitin binding, and antimicrobial activities. Both rMchi-F and rMchi-N displayed enzymatic activity with the optimum pH of 4.0 and optimum temperature of 40 °C, and rMchi-N showed a stronger activity than rMchi-F. Enzymatic activities of rMchi-F and rMchi-N were stimulated by the metal ions Fe^{2+}, Ba^{2+}, and Na^{+} and partially inhibited by Cu^{2+}, Ni^{2+} and Zn^{2+}. rMchi-F, rMchi-N, and sMchi-CB had the ability to combine with colloid chitin. The antimicrobial activities of these proteins were tested against bacteria and fungi, and the results indicated the strongest activity for sMchi-CB and the weakest activity for rMchi-N. Using a prepared anti-rMchi-F polyclonal antibody, immunohistochemistry and immunoprecipitation were performed and the results revealed the location of mytichitin-1 in mantle, digestive gland and blood cells. In addition, two forms of mytichitin-1, mytichitin-CB (6 kD) and full-length mytichitin-1 (48 kD), were detected, and a 35 kD protein was identified as the third form of mytichitin-1, existing in various tissues of *M. coruscus*. These findings suggest that mytichitin-1 may play different roles, with at least three forms, in different *M. coruscus* tissues.

1. Introduction

Marine molluscs are widespread and constantly under an enormous microbial challenge from the ocean environments. Antimicrobial peptides (AMPs) are the major components in molluscs for defending themselves against microorganisms in such conditions [1–5]. Most AMP studies of marine molluscs have focused on species of *Mytilus*, such as *M. californianus, M. edulis* and *M. galloprovincialis*, and the isolation and characterization of AMPs date back to 1996 [6,7]. Eight AMP families have been identified in *Mytilus*, including defensin [6], mytilin [8], myticin [9,10], mytimycin [11], mytimacin [12], big defencin [12], myticusin [13], and mytichitin-CB [14], which makes *Mytilus* a promising species containing abundant AMPs that could be used as leading molecules of antibacterial drugs.

A novel chitin-binding domain-containing AMP has been identified, as the C-terminal fragment of a chitinase-like protein named mytichitin-1, in *M. coruscus* serum [14]. Mytichitin-1 shows more than 35% sequential identity with chitinases from other species. Chitinases are a class of evolutionarily ancient enzymes with the function of chitin hydrolysis (endo-β-1,4-N-acetylglucosaminidases) and are found in chitin-containing organisms, as well as in widely diverse organisms without chitin. For example, in humans, despite the absence of endogenous chitin, two types of chitinase, chitotriosidase and acid mammalian chitinase, are reported [15–17]. The former functions as a host defence factor against chitin-coated pathogens and is the major chitinase measured in disease states [15,16], and the latter is acid stable and has a

* Corresponding author.
E-mail address: m13454066448@163.com (L. Zhi).

https://doi.org/10.1016/j.fsi.2018.10.081
Received 1 July 2018; Received in revised form 25 October 2018; Accepted 28 October 2018
Available online 03 November 2018
1050-4648/

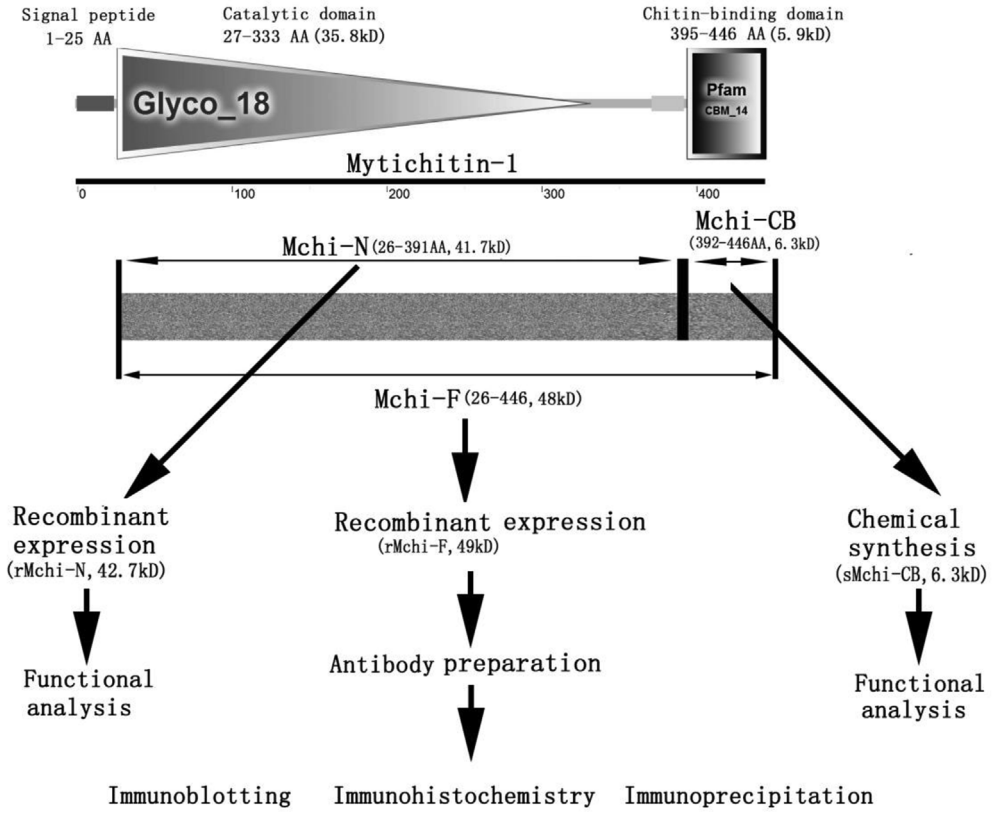

Figure 1. The predicted domain organization of mytichitin-1 precursor, the schematic view of the different regions for recombinant expression or chemical synthesis, and the flow chart of the experimental process in this study.

dual function in digestion of chitinous substrates and host defence [17]. In other organisms, chitinase performs diverse physiological functions, such as cell wall degradation and modification [18], insect moulting [19], hatching [20], early embryonic development [21], and immunity effectors [22].

In marine mussel *M. coruscus*, five chitinase-like genes (mytichitin-1 to 5 with the accession numbers AHC08445.2 and AIF74556.1–AIF74559.1, respectively) have been cloned [14]. Mytichitin-1 mRNA is expressed mainly in gonad and digestive gland and is upregulated in haemocytes in response to bacterial induction [14]. Furthermore, mytichitin-1 was also identified as one of shell matrix proteins in the proteomic analysis of *M. coruscus* shell [23]. These results indicate mytichitin-1 may participate in proliferation, digestion, immune, and shell formation. The full mytichitin-1 (Mchi-F in this article) consists of a large N-terminal catalytic domain and a small C-terminal chitin-binding domain (Fig. 1). As the C-terminal region of mytichitin-1, Mchi-CB shows strong antimicrobial activities against Gram-positive bacteria and fungi [14]. The organization and processing of an AMP from a large parental molecule is an efficient way to synthesize different effector molecules and/or amplify the antibacterial response, such as buforin I from histone H2A [24] and astacidin 1 from haemocyanin [25]. However, why and how Mchi-CB was removed from Mchi-F naturally in *M. coruscus* is unclear, and thus, functional comparison of the different regions from Mchi-F in detail is necessary. In this article, the full mature mytichitin-1 gene (*Mchi-F*) of *M. coruscus* and its N-terminal region gene (*Mchi-N*) were separately expressed in *Escherichia coli* BL21 with codon optimization. The Mchi-CB was produced by chemical synthesis. The three protein products were further analysed after purification and refolding. Functional comparisons between the three molecules and the location of mytichitin-1 in tissues will be useful and valuable for elucidating the molecular characteristics of mytichitin-1.

2. Material and methods

2.1. Recombinant expression of the Mchi-F and the Mchi-N gene

The full and the N-terminal region of mytichitin-1 gene (without the signal peptide sequence) were codon-optimized and synthesized for an *E. coli* expression system. An *Nco I* restriction site and a *Xho I* site were attached to the 5′ and 3′ ends of the optimized sequence, respectively. A 6x His tag was also added at the 5' end of the genes. The synthetic codon-optimized genes were excised by digestion with *Nco I* and *Xho I* and ligated into a pET28α expression vector (Invitrogen). The construct was designed to yield two protein products, 429 amino acids (AA) with molecule weight of ~49 kD for recombinant Mchi-F (rMchi-F) and 374 AA (~42 kD) for recombinant Mchi-N (rMchi-N), fused in frame with a 6x His tag (Figs. 1 and 2). The correct sequence of the expression plasmid was confirmed by DNA sequencing.

The recombinant proteins (rMchi-F and rMchi-N) were expressed in *E. coli* strain BL21. Cells were grown in LB Broth to optic density (OD_{600}) ≈0.7 at 37 °C, and protein expression was then induced by 1 mM isopropyl-D-thiogalactopyranoside (IPTG) at 37 °C for 4 h. Then, the cells were harvested by centrifugation (1000 × *g*, 10 min). Cell pellets were re-suspended in ice-cold lysis buffer (10 mM imidazole, 50 mM PBS, 100 mM NaCl, 1 M EDTA, pH 8.0) and then homogenized by sonication. The crude lysate was centrifuged at 8000 × *g* for 30 min at 4 °C. The precipitate was dissolved in buffer A (10 mM imidazole, 8 M urea, 100 mM NaCl, 100 mM PBS, pH 8.0), then applied to a Ni-NTA column and washed with buffer B (30 mM imidazole, 8 M urea, 100 mM NaCl, 100 mM PBS, pH 8.0) and buffer C (300 mM imidazole, 8 M urea, 100 mM NaCl, 100 mM PBS, pH 8.0), respectively, under ice-cold conditions.

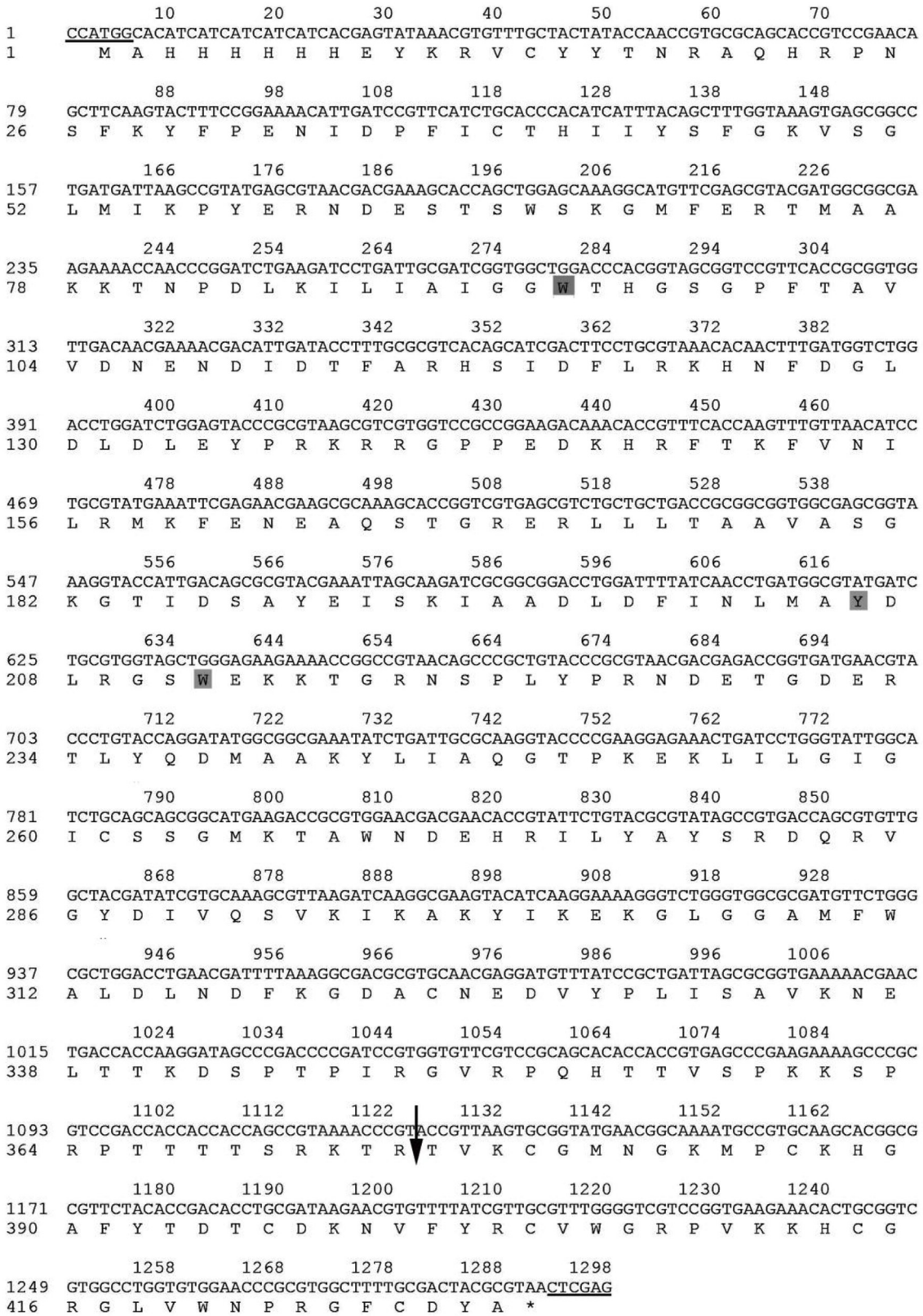

Figure 2. Sequence alignment of the optimized recombinant gene with the deduced amino acid sequence of mytichitin-1. The restriction endonuclease cleavage sites (*Nco I* and *Xho I*) were underlined at 5′ and 3′, respectively; the termination codon was denoted by "*"; the boundary between rMchi-N and Mchi-CB was denoted by an arrow in the sequence; three conserved aromatic amino acids (Trp and Tyr) corresponding to the key residues of possible chitin-binding sites (see Ref. [32]) located in the catalytic domain were shaded.

2.2. Chemical synthesis of Mchi-CB

The Mchi-CB with 55-AA was synthesized on an automated PerSeptive Biosystems Pioneer peptide synthesizer using the continuous flow Fmoc solid phase synthesis methodology. Synthesized Mchi-CB (sMchi-CB) was purified by high-performance liquid chromatography (HPLC, Waters 650E, USA) using a solvent system composed of a mixture of acetonitrile, trifluoroacetic acid, and water following the method used in our previous work [14]. The identity of the synthetic peptide was confirmed by electro-spray ionization mass spectrometry (ESI-MS). Synthetic peptide was dissolved in sterile deionized water at a concentration of 1 mM and stored at −20 °C before use.

2.3. Protein refolding, purification, electrophoresis, and Western blotting

For rMchi-F and rMchi-N samples, a series of dialysis steps was performed in buffers containing the oxidized and reduced glutathione (GSH/GSSG) in a graded of concentration of urea (1–8 M) to assist protein refolding according to the method reported previously [26]. All dialysis procedures were performed in a dialysis bag (1 kD) at 4 °C. Pooled fractions from the Nickel column were diluted to a final protein concentration of 0.5 mg/mL in buffer I with 8 M urea and dialyzed twice into buffer II containing 6 M urea. This sample was transferred to a fresh dialysis bag and dialyzed twice into buffer III containing 4 M urea, followed by 2 M urea buffer IV and 1 M urea buffer V using the same dialysis procedure. All buffers contained 0.1 mM GSSH, 0.9 mM GSH, and 20 mM Tris-HCl with a pH of 8.0. Finally, the protein sample was purified and desalted by HPLC (Waters 650E, USA) using a reverse-phase C4 column (Vydac, 208TP). The eluted protein fraction from HPLC was lyophilized and stored at −20 °C before use.

For sMchi-CB, the oxidative refolding was performed in GSH/GSSG buffer. Protein sample was dissolved (0.5 mg/mL) in a buffer (0.05 mM Tris-HCl, 0.05 M NaCl, 1.5 mM GSH, and 0.15 mM GSSG, pH 8.6) under stirring at 4 °C for 24 h. Reverse-phase HPLC (Waters 650E, USA) and MALDI-TOF mass spectrometry (4700 Proteomics Analyser, Applied Biosystems) were used to monitor the refolding process. Finally, the refolded peptides were purified by HPLC with a reverse-phase C18 column (Vydac, 218TP) and lyophilized for use.

SDS-PAGE was performed on a 12% polyacrylamide gel, and the protein bands were visualized using Coomassie Brilliant Blue R-250. Proteins were transblotted onto PVDF membranes and probed with a His-Tag monoclonal antibody (GenScript) and then incubated with HRP-conjugated secondary antibody as recommended by the manufacturer (GenScript). Immunoreactive bands were visualized using a Western blotting ECL kit (Solarbio, Beijing, China) according to the instructions provided by the manufacturer.

2.4. Enzymatic activity assays

Chitinase activity was measured using a classic 3,5-dinitrosalicylic acid (DNS) method. The reaction mixture contained 10% colloidal chitin (Sigma-Aldrich) in 50 mM PBS (pH 4.0) with enzyme solution. After incubation at 40 °C for 10–90 min, the reaction was terminated by boiling at 100 °C for 5 min. The reaction mixture was centrifuged at 12,000 × *g* for 5 min. DNS reagent was then added to the reaction mixture and boiled at 100 °C for 10 min. After cooling, the content of reducing sugars was measured according to the standard curve at 540 nm using a UV spectrophotometer. One unit (U) of chitinase activity was defined as the amount of enzyme that was required to release 1 μM of GlcNAc per min under the assay conditions. Protein content was measured according to the Bradford method using bovine serum albumin (BSA) as a protein standard.

The optimal temperature for enzymatic activity was determined by testing the hydrolysis of colloidal chitin as a substrate, under conditions described above. Temperatures tested ranged from 10 to 80 °C for 1 h. A temperature profile was produced with the enzyme activity at the optimum temperature set to 100%. For assessing the optimal pH activity, buffers at pH ranging from 3.0 to 10.0 (50 mM PBS buffer for pH 3.0–6.0 and 50 mM Na_2CO_3-$NaHCO_3$ buffer for pH 7.0–10.0) were used. Reactions were carried out using colloidal chitin at 40 °C for 1 h, and the enzyme activity at the optimum pH was set to 100%. All assays were performed in triplicate, and the mean values were used to plot each time or pH point.

Metal ions are generally considered important factors affecting chitinase enzyme activity. The reaction mixture consisted of purified enzyme in 100 mM citrate buffer (pH 4.0) containing 1 mM metal ions (K^+, Cu^{2+}, Mg^{2+}, Fe^{2+}, Fe^{3+}, Ni^{2+}, Ba^{2+}, Ca^{2+}, Na^+, Li^+, and Zn^{2+}). The effect of these metal ions was investigated using the chitinase assay system mentioned above. The system without any additives was used as a control and set to 100%.

2.5. Chitin-binding assays

The chitin-binding assay was performed as described by Kini et al. [27] with modification. Briefly, colloidal chitin was equilibrated in binding buffer (0.5 M NaCl, 10 mM Tris, 1.05% Triton X-100, pH 7.0). Protein samples were diluted as 0.25 mg/mL in 2.0 mL binding buffer. The protein solution was mixed with the colloidal chitin and incubated for 1 h at room temperature with gentle shaking. After incubation, the reaction mixture was centrifuged at 12,000 × *g* for 20 min. The supernatant (I) was then analysed by SDS-PAGE as described above. The precipitate (the remaining chitin) was washed three times using 0.1 M PBS buffer (pH 7.4). The bound protein sample was released using 10 mM phosphate buffer (pH 7.4) containing 8 M urea by centrifugation at 12,000 × *g* for 20 min. The supernatant (II) was analysed by SDS-PAGE.

2.6. Antimicrobial activity assays

Bacteria and fungi used in present study were the same strains used in a previous work [14] and were obtained from China General Microbiological Culture Collection Center (CGMCC, Beijing, China). Antimicrobial activity was monitored by a liquid growth inhibition assay according to the method described previously [14]. Pure water and natural mytichitin-CB [14] were used as negative and positive controls, respectively.

To determine the minimal inhibitory concentration (MIC), serial doubling dilutions were carried out following the protocols described by Mitta [9]. The MIC values are expressed as an interval (a–b), where “a” represents the highest peptide concentration tested at which bacteria were still growing and “b” the lowest concentration that caused 100% growth inhibition.

2.7. Polyclonal antibody preparation and immunoblotting analysis

The purified rMChi-F was enriched and submitted to Shanghai Qiangyao Biotechnology Company (Shanghai, China) to produce polyclonal antibody. Briefly, two male New Zealand rabbits were immunized subcutaneously with a mixture of 1 mg protein sample in 1 mL PBS buffer with an equal volume of complete Freund's adjuvant. Three booster injections each containing 1 mL rMChi-F (1 mg/mL) plus incomplete Freund's adjuvant (1 mL) were subsequently given at two week intervals. The antiserum was collected through the carotid artery 10 d after the last immunization and further purified by a protein A/G column. The titre for the antibody was detected by ELISA. The specificity against rMChi-F, rMchi-N, sMchi-CB, and total proteins extracted from six tissues of adult *M. coruscus* was tested by Western blotting using the anti-rMchi-F polyclonal antibody (1:2000) and rabbit anti-β-actin antibody (1:5000, HuaAn Biotechnology Co., Ltd). The secondary antibody was horseradish peroxidase-labelled goat anti-rabbit IgG (1:10,000; HuaAn Biotechnology Co., Ltd.). Blots were visualized using 3,3’,5,5’-tetramethylbenzidine stabilized substrate.

Using anti-rMChi-F polyclonal antibody, immunohistochemistry (IHC) assays were conducted on paraffin sections from experimentally infected tissues (mantle, digestive gland, and blood cell) to determine the tissue distribution of chitinase within *M. coruscus*. The mussels were induced by injection of bacteria (*E. coli* and *S. luteus* at a 1:1 ratio at 10^6 CFU). After induction for 12 h, the tissues were isolated and preserved in 10% formaldehyde for 24 h, and then, they were dehydrated through ascending grades of ethanol. The tissues were imbedded in paraffin, and 5 μm sections were cut using a microtome and were collected on coated slides for immunohistochemistry. The sections were deparaffinized in xylene and ethanol and further treated in a methanol bath containing 0.3% of hydrogen peroxide during 1 h in the dark at room temperature to inactive endogenous peroxidases. The non-specific interactions were blocked using 1% BSA for 20 min at room temperature. The slides were incubated overnight at 37 °C with the polyclonal primary antibody diluted in 1X PBS (1:200, pH 7.4), supplemented with 1% BSA. The primary antibodies were detected using a peroxidase-conjugated antibody against rabbit IgG and stained by DAB solution.

The mantle sampled at 12 h post-injection was used for further immuno-electron microscopy analysis. Briefly, small pieces of the mantle were processed for pre-embedding immunogold labelling with primary antibodies (rabbit anti-rMChi-F, diluted 1:100) and secondary antibodies (gold-labelled goat anti-rabbit). The labelled tissues were infiltrated with white acrylic resin after dehydration. The specimens were polymerized in the bottom of closed gelatine capsules filled with fresh LR white resin. Ultra-thin sections (70 nm) were picked and were counterstained with uranyl acetate and lead citrate for examination and photography with a transmission electron microscope (TECANI T10, 100Kv, PHILIPS).

2.8. Protein immunoprecipitation

Immunoprecipitation (IP) was performed using a Thermo Scientific™ Pierce™ Classic Magnetic IP/Co-IP Kit according to the protocols provided by the kit. Briefly, the protein-A/G magnetic beads (0.25 mg) were blocked by BSA and then used for antibody coupling. The rabbit polyclonal anti-rMChi-F antibodies were mixed with the protein-A/G magnetic beads for 1 h at room temperature. After binding of the antibodies, the beads were washed twice with IP Wash Buffer. The beads were then incubated with a whole lysate from *M. coruscus* mantle overnight at 4 °C in mild spin rotation in IP buffer. After washing three times with cold IP Wash Buffer, the beads were collected with a magnetic stand, and the immunoprecipitated antigens were solubilized in Lane Marker Sample Buffer, denatured at 96 °C for 10 min and separated by 12% SDS-PAGE. The stained bands were dissected, and the proteins inside the bands were submitted to LC-MS/MS (Triple TOF 5600, AB SCIEX) analysis after trypsin digestion. The trypsin-digested mixture of protein sample was separated on an Ekspert nanoLC 415 HPLC (SCIEX, Concord, ON) with a ChromXP C18 column (75 μm × 150 mm, 3.0 μ, 120 Å). The HPLC gradient was 8–38% buffer B (98% ACN, 0.1% formic acid) in buffer A (2% ACN, 0.1% formic acid) at a flow rate of 300 nL/min over 25 min. Isolated peptides from HPLC were submitted into the Triple TOF 5600 with Information Dependent Analysis (IDA) model detection, under the ion spray voltage of 2.4 kV. The MS data were acquired automatically, and the raw MS/MS data were converted into WIFF format for bioinformatics analysis. The proteins were identified by PEAKS Studio (version 8.5, Bioinformatics Solutions Inc. Waterloo, Canada) against the UniProt *Pteriomorphia* protein database. Carbamidomethyl (C) was set as a fixed modification. Oxidation (M), Gln- > pyro-Glu (N-term Q), and Deamidated (NQ) were set as variable modifications. The Peptide Mass Tolerance was set to 20 ppm, and the Fragment Mass Tolerance was set to 0.05 Da, respectively. False discovery rate (FDR) analysis was performed, and FDR < 0.05 was considered for protein identification by using the target-decoy search strategy.

3. Results

3.1. Expression, purification, and refolding of rMchi-F and rMchi-N

The open reading frame of native myticitin-1 cDNA encodes a 446-AA precursor including with a 25-AA signal peptide. The domain structure of myticitin-1 precursor was predicted by SMART (http://smart.embl-heidelberg.de/). The sequence of myticitin-1 comprised a Glyco_18 domain and a chitin-binding (CBM_14) domain (Fig. 1). We also show the experimental flow chart in the same figure. The native genes of *Mchi-F* and *Mchi-N* were codon-optimized to adjust to the most preferred triplets in *E. coli* strains. The optimization did not change the amino acid sequence (Fig. 2). The sequence alignments of native mytichitin-1 (GenBank accession KF675770) with the codon-optimized genes (*rMchi-F* and *rMchi-N*), and the results of relative codon frequency before and after optimization are shown in Supplementary Fig. S1 and S2, respectively.

rMchi-F and rMchi-N were produced by a pET-28α/*E. coli* expression system with IPTG induction. SDS-PAGE (12%) analysis revealed the presence of rMchi-F and rMchi-N with the expected molecular weights (~49 for rMchi-F and ~42 kDa for rMchi-N) of the fusion proteins (with His-Tag) in the pellet fraction of *E. coli* lysates (Fig. 3A and C), which were further confirmed by Western blotting with anti-His-Tag antibody (Fig. 3 B and D). The expression levels of rMchi-F and rMchi-N were both estimated as 40 mg/L culture, by calculating the OD value of the standard BSA band loaded in SDS-PAGE (lane PC1 and PC2 of Fig. 3) and comparing these with the OD values of the bands from rMchi-F and rMchi-N in the same gel. The recombinant His-tagged proteins were purified by affinity chromatography with a nickel column from the pellet fraction of *E. coli* lysates. Using a GSH/GSSH oxidation buffer containing urea, the recombinant proteins were refolded stepwise by dialyses against a series of urea concentrations from high to low. Refolded proteins were then purified by reverse-phase HPLC using a C4 column (Supplementary Figure S3A) and analysed by LC-MS/MS (Supplementary Figure S3B). The sequences of the peptide fragments detected in LC-MS/MS completely matched the predicted N-terminal sequences of rMchi-F (124–137 AA of "-HNFDGLDLDLEYPR-" and 194–209 AA of "-IAADLDFINLMAYDLR-") and rMchi-N (124–138 AA of "-HNFDGLDLDLEYPRK-") (Supplementary Figure S3B), indicating that the sequence of recombinant proteins had been expressed correctly.

3.2. Purification and oxidation of sMchi-CB

sMchi-CB was purified by reverse-phase HPLC with a C18 column to > 95% purity (Supplementary Fig. S4A), and the identity of the synthetic peptide was confirmed by MS (Supplementary Fig. S4B). To obtain a cyclic peptide with disulphide bridges, we used a direct oxidation method in which the peptide containing six unprotected cysteines was allowed to form disulphides under oxidizing conditions. The refolded peptide was purified by reverse-phase C18 HPLC and analysed by MALDI-TOF. As shown in Supplementary Fig. S5A, the elution time of oxidized sMchi-CB in HPLC purification was advanced after oxidative refolding, and the MALDI-TOF analysis further confirmed that the molecular weight of sMchi-CB decreased by 7 Da after the refolding reaction for 24 h (Supplementary Fig. S5B).

3.3. Enzymatic and chitin-binding activity

Both rMchi-F and rMchi-N showed clear chitinase activity (Fig. 4), and no chitinase activity was detected for sMchi-CB (data not shown). The results of the time course experiments of substrate hydrolysis indicated that rMchi-F and rMchi-N had similar hydrolysing abilities towards the colloidal chitin. Compared with rMchi-F, rMchi-N showed a stronger activity (~60% of the maximal activity of rMchi-N was detected for rMchi-F.) (Fig. 4A). Both rMchi-F and rMchi-N showed chitinase activity from 20 to 80 °C (Fig. 4B), with the optimal

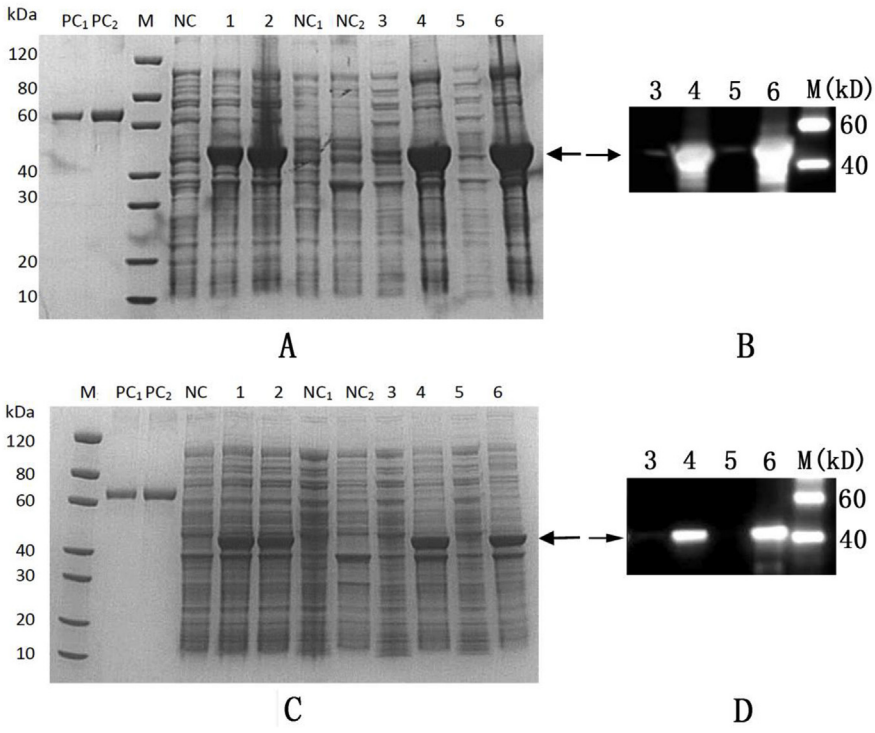

Fig. 3. SDS-PAGE with coomassie blue staining of rMchi-F (A) and rMchi-N (C), and western blot analysis of rMchi-F (B) and rMchi-N (D). M: protein standard marker; lane PC1, BSA (1 μg); lane PC2, BSA (2 μg); lane NC, cell lysate of blank control; lane NC1, soluble supernatant fraction from cell lysate without IPTG induction; lane NC2, insoluble cell debris fraction from cell lysate without IPTG induction; lane 1, cell lysate from IPTG induction at 15 °C for 16 h; lane 2, cell lysate from IPTG induction at 37 °C for 4 h; lane 3, soluble supernatant fraction from cell lysate of induction at 15 °C for 16 h; lane 4, insoluble cell debris fraction of cell lysate from induction at 15 °C for 16 h; lane 5, soluble supernatant fraction from cell lysate of induction at 37 °C for 4 h; lane 6, insoluble cell debris fraction of cell lysate from induction at 37 °C for 4 h. Arrows refer to the target protein with ~49 kDa for rMchi-F and ~42kD for rMchi-N.

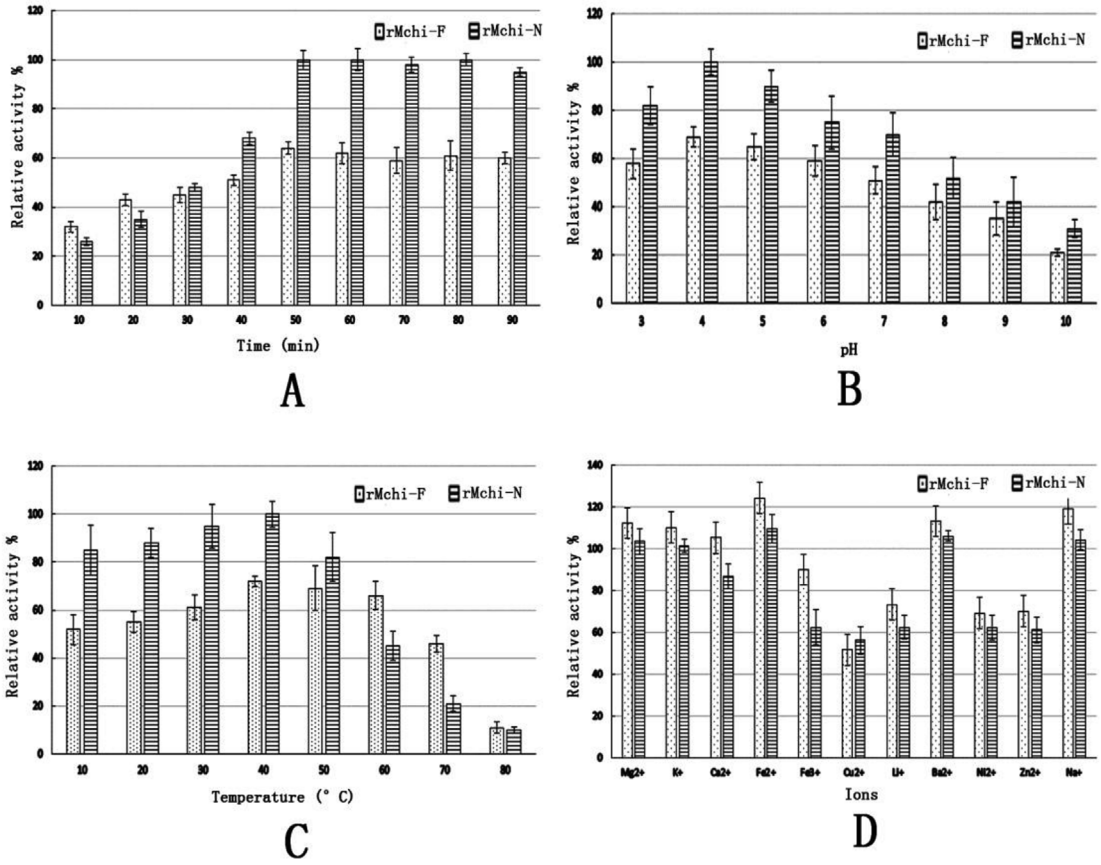

Fig. 4. Chitinase activities of rMchi-F and rMchi-N. A: the time course of chaitinase activity of rMchi-F and rMchi-N. Enzyme activity was determined at pH of 4.0 and temperature of 40 °C, and using colloidal chitin as substrate. The highest chitinase activity was set to 100%. **B:** effect of pH on chitinase activity. Enzyme activity was determined at a range of pH (3–10) and the temperature of 40 °C, and the highest chitinase activity was set to 100%. **C:** effect of temperature on chitinase activity. Enzyme activity was determined at a range of temperature (10–80 °C) and the pH of 4.0, and the highest chitinase activity was set to 100%. **D:** effect of metal ions on the chitinase activity of rMchi-F and rMchi-N. Enzyme activity was determined at temperature of 40 °C. No addition (with no metals added to the enzyme solutions) was used for 100% relative activity. Data were represented by the average value of three independent experiments. Error bars indicate standard deviation.

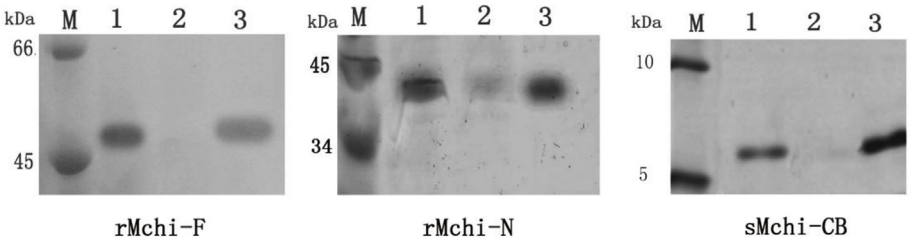

Figure 5. Chitin-binding activity of rMchi-F, rMchi-N, and sMchi-CB. Chitin-binding activity was tested by SDS-PAGE with Cormas Brilliant Blue staining. 12% SDS-PAGE was used for rMchi-F and rMchi-N, and 15% SDS-PAGE for sMchi-CB. Lane 1: purified protein sample; lane 2: the supernatant from centrifugation after incubation of protein sample with chitin; lane 3: the supernatant from centrifugation of urea treatment precipitates after incubation of protein sample with chitin.

temperature of 40 °C. Above 60 °C, the activity of rMchi-N decreased faster than that of rMchi-F, indicating greater thermo-stability of the latter. Both rMchi-F and rMchi-N showed chitinase activity from pH 3.0 to 10.0, with the optimum pH of 4.0 (Fig. 4C). The chitinase activity of rMchi-F and rMchi-N was increased by Fe^{2+}, Ba^{2+}, and Na^{+} and decreased by Cu^{2+}, Zn^{2+}, and Ni^{2+} (Fig. 4D).

The results of the chitin-binding assay showed that rMchi-F and sMchi-CB had significant chitin-binding abilities towards the colloidal chitin, and rMchi-N also retained a weaker ability towards colloidal chitin (Fig. 5).

3.4. Antimicrobial activity

The activity spectra of rMchi-F, rMchi-N, sMchi-CB, and natural mytichitin-CB were investigated against a variety of microorganisms (Table 1). In the liquid growth inhibition assays, both sMchi-CB and natural mytichitin-CB had strong activity against the Gram-positive bacteria (MIC < 10 μM) and fungi (MIC < 30 μM) and weak effects on the Gram-negative bacteria (MIC > 60 μM). Compared to sMchi-CB, rMchi-F showed a moderate antimicrobial activity, and rMchi-N showed the weakest activity among the tested samples.

3.5. Immunoblotting and immunoprecipitation

Using the anti-rMchi-F polyclonal antibody, we tested the protein expression in mantle, adductor muscle, gonad, digestive gland, serum, and blood cells of *M. coruscus*. As shown in Fig. 6, rMchi-F, rMchi-N, and sMchi-CB were detected specifically by anti-rMchi-F polyclonal antibody with the expected molecular sizes (49 kD for rMchi-F, 42 kD for rMchi-N, and 6 kD for sMchi-CB). In six tissues from *M. coruscus*, however, no ~42 kD band was detected; instead, a 35 kD band was specifically detected in the mantle, adductor muscle, gonad, digestive gland, and blood cell (Fig. 6), indicating that Mchi-N is not a native form of mytichitin-1 in *M. coruscus*. A 48 kD band was specifically detected in gonad and adductor muscle (Fig. 6), suggesting the presence of native mytichitin-1 in *M. coruscus*. In addition, a 6 kD band was specifically detected in the serum (Fig. 6), which was consistent with the fact that Mchi-CB had been identified in *M. coruscus* serum previously [14].

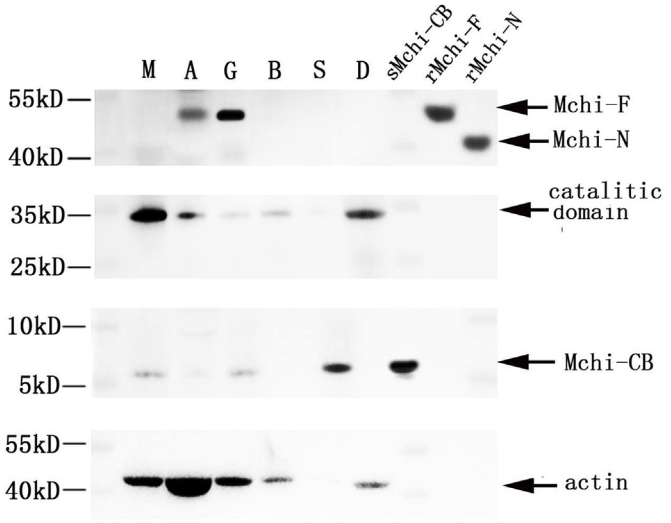

Figure 6. immunoblotting analysis of rMchi-F, rMchi-N, and sMchi-CB on six tissues of *M. coruscus*. Total proteins were collected from six tissues of *M. coruscus* and subjected to SDS-PAGE, and then analyzed by Western blotting with anti-rMchi-F antibody and goat anti rabbit IgG-HRP as indicator. M, mantle; A, adductor muscle, G, gonad; B, blood cells; S, serum; D, digestive gland. The specificity of anti-rMchi-F antibody was confirmed by purified rMchi-F (~49 kD), rMchi-N (~42 kD), and sMchi-CB (~6 kD), respectively, and indicated by arrows. The rabbit anti-actin polyclonal antibody (HuaAn Biotechnologigy Co., Ltd, Hangzhou, China) was used as control.

The 35 kD band was further detected by protein immunoprecipitation (Fig. 7A). The target antigen with 35 kD immunoprecipitated by anti-rMchi-F polyclonal antibody was identified by LC-MS/MS as a mytichitin with the accession A0A075M2L3_MYTCO (Fig. 7B).

3.6. Immunohistochemistry

IHC results from the three tissues sampled at 12 h post-injection are shown in Fig. 8. Compared with the tissues before challenge, the positive signal strength (brown colour) was significantly increased after

Table 1
Activity spectra of rMchi-F, rMchi-N, sMchi-CB, and natural mytichitin-CB against bacteria and fungus. The pure water was used as negative control.

Organisms	rMchi-F(μM)	rMchi-N(μM)	sMchi-CB(μM)	natural Mchi-CB(μM)
Bacteria:gram-negative				
Escherichia coli (CGMCC1.1583)	125.0–250.0	> 500	62.5–125.0	62.5–125.0
Vibrio Parahaemolyticus (CGMCC1.1616)	62.5–125.0	> 500	62.5–125.0	62.5–125.0
Pseudomonas aeruginosa (CGMCC1.0102)	31.3–62.5	125.0–250.0	31.3–62.5	31.3–62.5
Vibrio.harveyi (CGMCC1.1601)	31.3–62.5	250–500.0	31.3–62.5	125.0–250.0
Bacteria:gram-positive				
Bacillus subtilis (CGMCC1.1630)	3.9–7.8	15.6–31.3	1.9–3.9	1.9–3.9
Staphylococcus aureus (CGMCC1.128)	15.6–31.3	62.5–125.0	15.6–31.3	3.9–7.8
Sarcina luteus (CGMCC28001)	7.8–15.6	31.3–62.5	3.9–7.8	1.9–3.9
Bacillus megaterium (CGMCC1.1487)	7.8–15.6	31.3–62.5	3.9–7.8	3.9–7.8
Fungus				
Candida albicans (CGMCC2.2086)	7.8–15.6	31.3–62.5	1.9–3.9	7.8–15.6
Monilia albican (CMCC(F)98001)	15.6–31.3	31.3–62.5	3.9–7.8	15.6–31.3

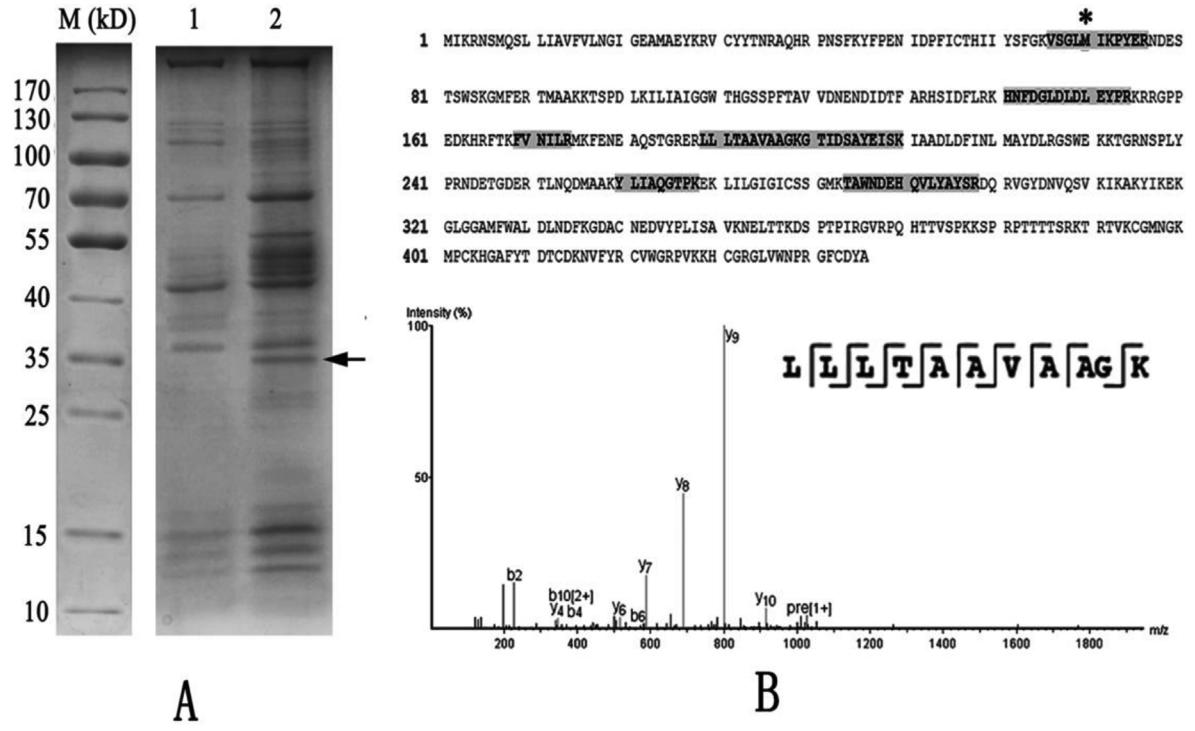

Figure 7. Protein immunoprecipitation (A) and target protein identification by LC-MS/MS (B). M, protein standard. Lane 1, immunoprecipitation by control rabbit IgG from the total proteins of mantle. Lane 2, immunoprecipitation by anti-rMchi-F polyclonal antibody from the total proteins of mantle. The target antigen with 35 kD immunoprecipitated by anti-rMchi-F polyclonal antibody was denoted by an arrow. The 35 kD band was further dissected and submitted to LC-MS/MS analysis. Seven peptides (shaded sequences) were identified as the fragments from the N-terminal of mytichitin (A0A075M2L3_MYTCO) with FDR < 0.05. A represent MS/MS spectrum was shown with the peptide coverage (upper panel) and the represent peptide sequence of "–LLLTAAVAAGK-" (lower panel). *represents the oxidation site of Met residue.

bacterial injection, indicating that mytichitin-1 was upregulated in all of the tested tissues after bacterial induction. In the mantle, IHC for mytichitin-1 showed strong positive immunoreactivity in the epithelial cells at the edge of the mantle groove (Fig. 8A and B). In the digestive gland, the immune-positive signal was focused on the tube wall (Fig. 8C and D). In the blood cells, the immune-positive signal was comparatively weak before bacterial injection, and increased immunoreactivity was observed mainly at the cell membrane (Fig. 8E and F).

The edge of the mantle groove was selected for further immunoelectron microscopy analysis. Two types of cell were observed in the epithelium of mantle tissue, including small cone-shape cell and big round-shape cell (Fig. 9A). For the small cone-shape cell, immunoelectron microscopy of mytichitin-1 revealed the presence of gold particle-labelled signals near to the cell membrane and in the extracellular matrix (Fig. 9B). For the big round-shape cell, abundant mitochondria was observed and the presence of gold particle-labelled signals was mainly presented in the cytoplasm (Fig. 9C), especially near to the Golgi complex (Fig. 9D) and the outside of mitochondria (Fig. 9E). In addition, the gold particles were also presented near to the cell membrane and the extracellular matrix (Fig. 9F).

4. Discussion

The organization and processing of antimicrobial peptides from one larger precursor molecule is an efficient way to synthesize different effector molecules and amplify the antibacterial response. Examples include buforin I from the cytoplasmic histone H2A [24], astacidin 1 from haemocyanin [25], mouse α-defensin from metalloproteinase [28], and human defensin-5 from trypsin [29]. In a previous study, Mchi-CB with 55-AA containing a chitin-binding domain was purified from *M. coruscus* serum as an antimicrobial peptide. The sequence of Mchi-CB perfectly matches the C-terminus of mytichitin-1, indicating that Mchi-CB is released from the C-terminal region of mytichitin-1 via protein cleavage. In this study, we further demonstrated the chitin-binding ability and the presence of Mchi-CB in the serum by chitin-binding assay and immunoblotting, respectively. However, the destiny of the remainder of mytichitin-1 after removal of Mchi-CB is totally unclear. To explore the different roles played by the various regions of the mytichitin-1 molecule, the full-length and the N-terminal region of mytichitin-1 were recombinantly expressed separately. Together with the chemosynthetic Mchi-CB, the three protein products were functionally analysed and compared in the present study.

Both rMchi-F and rMchi-N showed significant chitinase activity with similar optimum pH and temperatures in this study (Fig. 4), and no chitinase activity was detected for sMchi-CB (data not shown). The catalytic activity of rMchi-F and rMchi-N was affected by the addition of various metal ions. Considering that *M. coruscus* is a mussel that lives in the sea, it is not surprising that the metal ions that rich in seawater, such as Na^+, Mg^{2+}, Ba^{2+}, and Fe^{2+}, can stimulate its enzymatic activity. However, the chitinases from different species may be stimulated or inhibited by different ions, and the mechanisms of their effects are still unknown. Compared with rMchi-F, rMchi-N showed a slightly stronger enzymatic activity for colloid chitin, which is probably due to the removal of the steric hindrance region (Mchi-CB) that may lower the accessibility of substrate to the catalytic site of mytichitin-1. This phenomenon is not peculiar, as some chitinases without C-terminal chitin-binding domains still have strong enzymatic activity on the chitin substrate [30]. Interestingly, rMchi-N showed chitin-binding activity despite lacking the chitin-binding domain (Fig. 5). The exposed aromatic residues, such as Trp and Tyr, of chitinase are important and strongly related to the insoluble chitin-binding and hydrolysis ability [31,32]. Sequence alignments among mytichitin-1 and other chitinases showed that these aromatic residues were also conserved in the catalytic domains (data not shown). Although mytichitin-1 has a chitin-

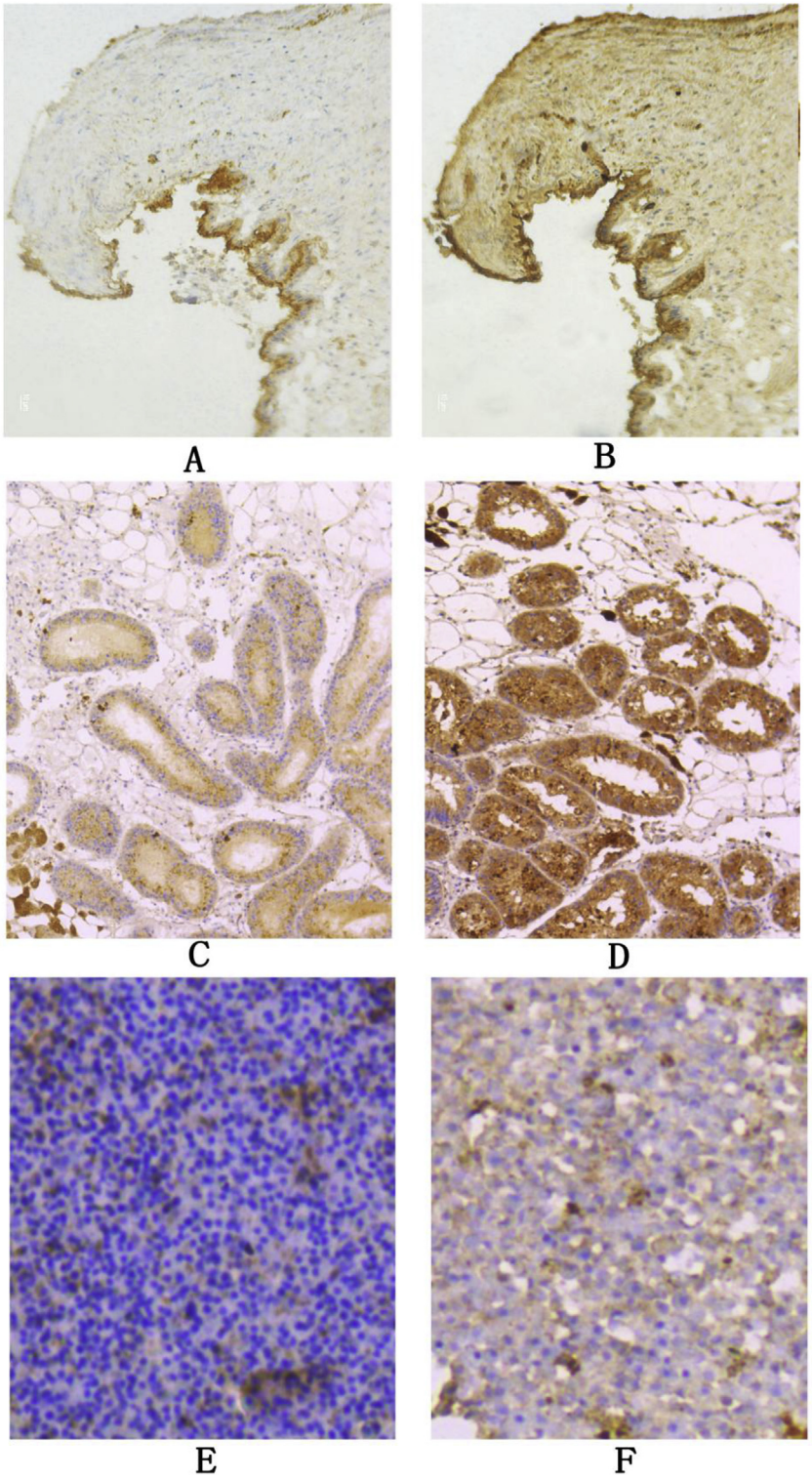

Fig. 8. Immunohistochemistry of mytichitin-1 detected by anti-rMchi-F polyclonal antibody in mantle, digestive gland, and blood cells of *M. coruscus*. **A**: expression of mytichitin (brown color) in mantle before bacteria induction. **B**: expression of mytichitin (brown color) in mantle after bacteria induction. **C**: expression of mytichitin (brown color) in digestive gland before bacteria induction. **D**: expression of mytichitin (brown color) in digestive gland after bacteria induction. **E**: expression of mytichitin (brown color) in blood cells before bacteria induction. **F**: expression of mytichitin (brown color) in blood cells after bacteria induction. (× 100). (For interpretation of the references to color in this figure legend, the reader is referred to the Web version of this article.)

binding domain in its C-terminus, it is still possible that the catalytic domain of mytichitin-1 (rMchi-N, for example) can interact with chitin substrate via the conserved aromatic residues located in the N-terminal region, such as Trp93, Tyr206 and Trp212 (Fig. 2), corresponding to the key conserved Trp164, Tyr279 and Trp285 of *Bacillus circulans* chitinase A1 for chitin-binding [32]. Therefore, in rMchi-N, the removal of the chitin-binding domain did not eliminate the abilities of insoluble chitin-binding and hydrolysis. However, opposite results have been reported for some chitinases from other species, in which the chitin-binding domain has a significant effect on the enzymatic and chitin-binding activities [33–35]. These opposite results indicate that the role of the chitin-binding domain in chitinase is more complex than people have imagined, and the results of functional analyses of various regions of chitinases are still too diverse to draw a simple conclusion.

Mytichitin-CB is an antimicrobial peptide from *M. coruscus* [14]. In this study, the synthesized mytichitin-CB (sMchi-CB) showed a similar antimicrobial activity to the natural form (Table 1). The antimicrobial activity of rMchi-F was significantly decreased compared to the mytichitin-CB, and the antimicrobial activity of rMchi-F was the weakest. These results indicate that the chitin-binding domain (mytichitin-CB) is

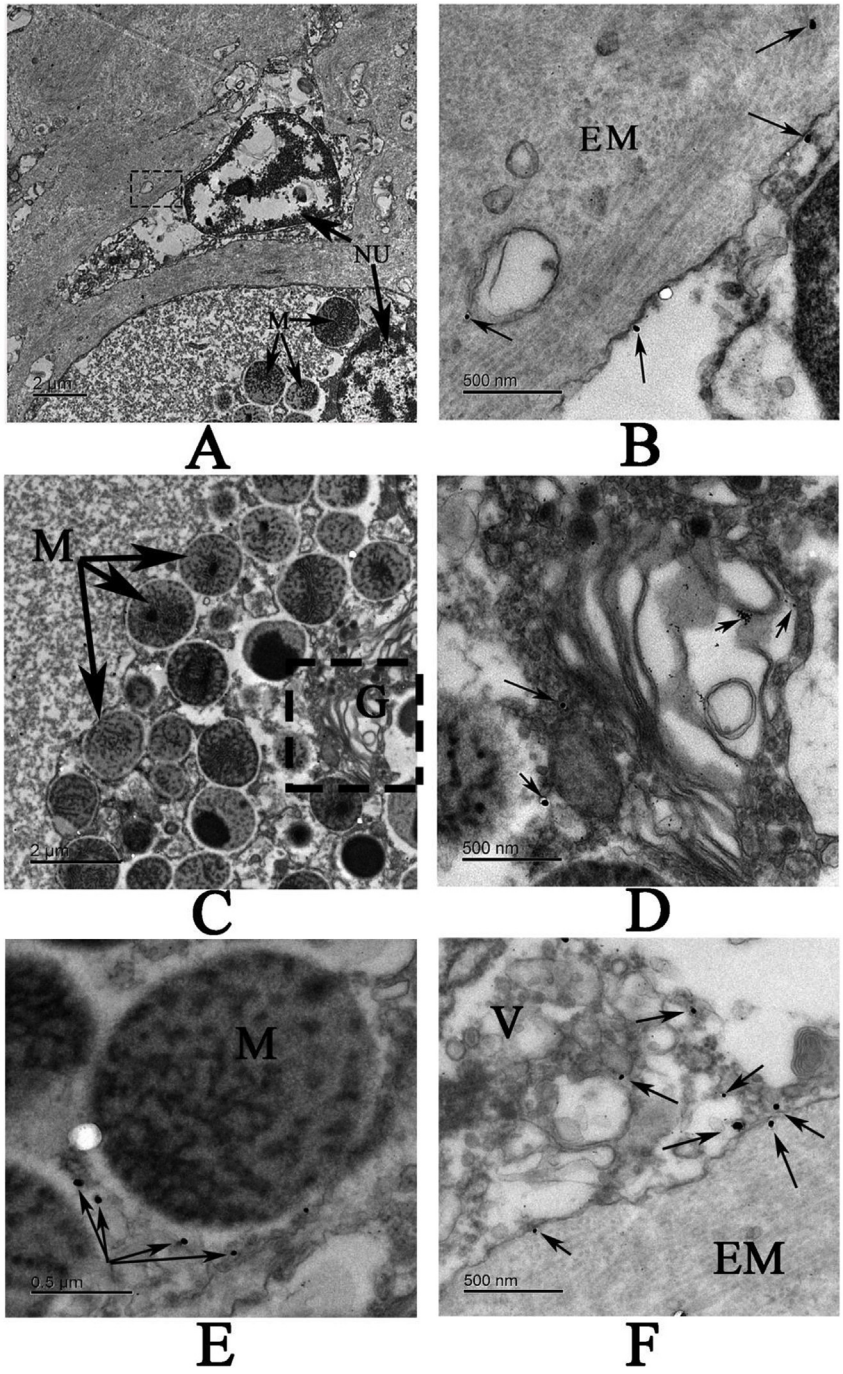

Fig. 9. Immuno-electron photomicrographs of the epithelium of *M. coruscus* mantle tissue. **A**: electron photomicrograph of a part of epithelium with two type of cells presented. **B**: enlarged electron photomicrograph of the region surrounded by dashed line in A and the presence of gold particles (denoted by arrows) near to the membrane region. **C**: electron microscopy of cytoplasm of the round-shape cell with abundant mitochondrion. **D**: enlarged electron photomicrograph of the region surrounded by dashed line in C and the presence of gold particles (denoted by arrows) near to the Golgi complex. **E**: the gold particles (denoted by arrows) presented in the outside of mitochondrion. **F**: the gold particles (denoted by arrows) presented in the cell membrane region of the round-shape cell. NU, nucleus; M, mitochondrion; EM, extracellular matrix; G, Golgi complex; V: vesicle.

the main contributor to the antimicrobial activity. It is postulated that chitinase can interact with the chitin of the cell wall of microorganisms and thus shows antimicrobial activity [18], suggesting the important roles of the chitin-binding domain in the antimicrobial activity. However, the mode of action of chitin-binding antimicrobial peptides is still poorly understand for now. In rMchi-F, the catalytic domain may impede this interaction, and in rMchi-N, the lack of a chitin-binding domain makes this molecule lose most of the antimicrobial activity. Furthermore, as an immune factor, the expression level of the mytichitin-CB gene can be stimulated by bacterial induction [14]. In this study, we observed that the protein expression level of mytichitin-1 detected by anti-rMchi-F antibody increased in mantle, digestive glands, and blood cells of *M. coruscus* after bacterial induction. The location of expressed mytichitin-1 is mainly in the epidermal layer of mantle, the tube wall of digestion glands, and the cytoplasm of blood cells (Fig. 8). In addition, the localization of mytichitin-1 in the mantle epidermal layer after bacterial induction was mainly presented in the cytoplasm, including Golgi complex, the cell membrane, and the extracellular matrix (Fig. 9). These results suggest mytichitin-1 is an immune-related protein that can be secreted and released from the tested tissues after bacterial induction. However, using only the anti-rMchi-F antibody, we could not discriminate which form mytichitin-1 may adopt for dealing with the stimulation because all three protein forms (Mchi-F, Mchi-N, and Mchi-CB) can be recognized by the anti-rMchi-F antibody.

The molecular structures of chitinases must be diverse to meet the numerous, highly specific catalytic or other functional requirements. Therefore, the fact that one chitinase may present different forms with different functions is an economical way to use a single gene to produce diverse products to meet different functional requirements. In the present study, sMchi-CB showed the strongest antimicrobial activity

and rMchi-N showed the strongest enzymatic activity among the three molecules, suggesting Mchi-CB and Mchi-N may have greater abilities for immune and chitin digestion, respectively, compared with the parental mytichitin-1. In addition, the immunoblotting analysis showed that the anti-rMchi-F antibody recognized, out of the total proteins of various tissues, a 35 kD protein band (Fig. 6), which is almost the same as the predicted molecular size of the catalytic domain of mytichtin-1 (27–333 AA with 35.8 kD, Fig. 1). The 35 kD band was further detected by protein immunoprecipitation and explicitly identified as a mytichitin (Fig. 7). Interestingly, in the protein identification of the 35 kD band, all of the peptides identified by LC-MS/MS were distributed in the N-terminal 66–298 AA fragment, which were included in the catalytic domain (27–333 AA fragment, Fig. 1) of mytichitin-1. The similar molecular weights and the protein identification indicate the possibility that the 35 kD protein is the catalytic domain of mytichitin-1. Together with the 6 kD band (Mchi-CB) detected in *M. coruscus* serum by anti-rMchi-F antibody (Fig. 6), these observations strongly suggest that mytichitin-1 may exist as at least two forms in *M. coruscus* and that each form has a different biological function and location in *M. coruscus*, i.e., one as an enzyme for chitin degradation in various tissues (the N-terminal catalytic region with 35.8 kD) and the other as an antimicrobial peptide (Mchi-CB), at least in serum. More than that, the intact mytichtin-1 (~48 kD) was also detected by immunoblotting in gonad (Fig. 6). Considering that the mRNA of mytichitin-1 has been detected with the maximum expression level in gonad [14], it can be speculated that mytichitin-1 might present as the third form, *i.e.*, intact form, at least in the gonad. From these results, we believe that these various forms of mytichitin-1 may play specific roles individually in different tissues.

Chitinases translated from one gene with different lengths and weights have been reported previously [36–38]. Post-translational modification of chitinase precursors may occur at either the N-terminus [39] or C-terminus [37]. Post-translational processing of a chitinase could make the enzyme more suitable for meeting various requirements in their own environments [40], for efficient translocation through the cell membrane [41], or for protection from protease attack in the natural environment [30]. However, knowledge concerning the origin and post-translational processing of these chitinases is still poor. For mytichitin-1, although the parental mytichitin-1 and its two truncated derivatives were produced and functionally analysed in this work, the proteolytic process of mytichtin-1 and the real functions and locations of these derivatives are not yet totally understood. The exact mechanisms of these different forms of chitinase in their biological roles would have to be determined before final conclusions could be made.

Acknowledgements

This research was supported by the National Natural Science Fund of China (31671009, 41606418), Xinmiao Project of Zhejiang province (2017R411010), and the Public Welfare Project of Zhejiang province (2015C31003).

Appendix A. Supplementary data

Supplementary data to this article can be found online at https://doi.org/10.1016/j.fsi.2018.10.081.

References

[1] J.A. Tincu, S.W. Taylor, Antimicrobial peptides from marine invertebrates, Antimicrob. Agents Chemother. 48 (2004) 3645–3654.
[2] J.L. Dimarcq, P. Bulet, C. Hetru, J. Hoffmann, Cysteine-rich antimicrobial peptides in invertebrates, Biopolymers 47 (1998) 465–477.
[3] G. Arenas, F. Guzmán, C. Cárdenas, L. Mercado, S.H. Marshall, A novel antifungal peptide designed from the primary structure of a natural antimicrobial peptide purified from *Argopecten purpuratus*, Peptides 30 (2009) 1405–1411.
[4] M. De Zoysa, I. Whang, L. Youngdeuk, L. Sukkyoung, J.S. Lee, J. Lee, Defensin from disk abalone *Haliotis discus discus*: molecular cloning, sequence characterization and immune response against bacterial infection, Fish Shellfish Immunol. 28 (2010) 261–266.
[5] P. Bulet, J.L. Dimarcq, C. Hetru, M. Lagueux, M. Charlet, G. Hegy, Antimicrobial peptides: from invertebrates to vertebrates, Inmmunol. Rev 198 (2004) 169–184.
[6] F. Hubert, T. Noel, P. Roch, A member of the arthropod defensin family from edible Mediterranean mussels (*Mytilus galloprovincialis*), Eur. J. Biochem. 240 (1996) 302–306.
[7] M. Charlet, S. Chernysh, H. Philippe, Innate immunity. Isolation of several cysteine-rich antimicrobial peptides from the blood of a mollusk, *Mytilus edulis*, J. Biol. Chem. 271 (1996) 21808–21813.
[8] G. Mitta, F. Vandenbulcke, F. Hubert, Involvement of mytilins in mussel antimicrobial defense, J. Biol. Chem. 275 (2000) 12954–12962.
[9] G. Mitta, F. Hubert, T. Noel, Myticin, a novel cysteine-rich antimicrobial peptide isolated from hemocytes and plasma of the mussel *Mytilus galloprovincialis*, Eur. J. Biochem. 265 (1999) 71–78.
[10] A. Pallavicini, M. del Mar Costa, C. Gestal, R. Dreos, A. Figueras, P. Venier, et al., High sequence variability of myticin transcripts in hemocytes of immunestimulated mussels suggests ancient host-pathogen interactions, Dev. Comp. Immunol. 32 (2008) 213–226.
[11] F. Cantet, M. Toubiana, M.G. Parisi, M. Sonthi, M. Cammarata, P. Roch, Individual variability of mytimycin gene expression in mussel, Fish Shellfish Immunol. 33 (2012) 641–644.
[12] G. Marco, D.M. Gianluca, M. Chiara, V. Paola, P. Alberto, Big defensins and mytimacins, new AMP families of the Mediterranean mussel *Mytilus galloprovincialis*, Dev. Comp. Immunol. 36 (2012) 390–399.
[13] Z. Liao, X.C. Wang, H.H. Liu, M.H. Fan, J.J. Sun, W. Shen, Molecular characterization of a novel antimicrobial peptide from *Mytilus coruscus*, Fish Shellfish Immunol. 34 (2013) 610–616.
[14] C.L. Qin, W. Huang, S.Q. Zhou, X.C. Wang, H.H. Liu, M.H. Fan, Characterization of a novel antimicrobial peptide with chiting-binding domain from Mytilus coruscus, Fish Shellfish Immunol. 41 (2014) 362–370.
[15] R.G. Boot, G.H. Renkema, M. Verhoek, A. Strijland, J. Bliek, T.M. de Meulemeester, The human chitotriosidase gene. Nature of inherited enzyme deficiency, J. Biol. Chem. 273 (1998) 25680–25685.
[16] L. Malaguarnera, R.M. Di, M.D. Rosa, A.M. Zambito, N. Dell'Ombra, M.R. Di, Potential role of chitotriosidase gene in nonalcoholic fatty liver disease evolution, Am. J. Gastroenterol. 107 (2012) 2060–2069.
[17] S. Adrangi, M.A. Faramarzi, From bacteria to human: a journey into the world of chitinases, Biotechnol. Adv. 31 (8) (2013) 1786–1795.
[18] C. Alfonso, M.J. Martínez, F. Reyes, Purification and properties of two endochitinases from Mucor rouxii in its cell wall degradation, FEMS Microbiol. Lett. 95 (1992) 187–194.
[19] K.J. Kramer, S. Muthukrishnan, Insect chitinases: molecular biology and potential use as biopesticides, Insect Biochem. Mol. Biol. 27 (1997) 887–900.
[20] C.M. Zhang, WuX, X.H. Cai, Effect of chitinases produced by Pochonia chlamydosporia on egg-hatching of Meloidogyne incognita, Sci. Agric. Sin. 42 (2009) 3509–3515.
[21] Z. Teng, S. Chen, S. Liu, H. Wang, S. Zhang, Functional characterization of chitinase-3 reveals involvement of chitinases in early embryo immunity in zebrafish, Dev. Comp. Immunol. 46 (2014) 489–498.
[22] H.T. Tran, N. Barnich, E. Mizoguchi, Potential role of chitinases and chitin-binding proteins in host-microbial interactions during the development of intestinal inflammation, Histol. Histopathol. 26 (11) (2011) 1453–1464.
[23] Z. Liao, L.F. Bao, M.H. Fan, P. Gao, X.X. Wang, C.L. Qin, X.M. Li, In-depth proteomic analysis of nacre, prism, and myostracum of Mytilus shell, J. Proteomics 122 (2015) 26–40.
[24] H.S. Kim, H. Yoon, I. Minn, C.B. Park, W.T. Lee, M. Zasloff, S.C. Kim, Pepsin-mediated processing of the cytoplasmic histone H2A to strong antimicrobial peptide buforin I, J. Immunol. 165 (2000) 3268–3274.
[25] S.Y. Lee, B.L. Lee, K. Söderhäll, Processing of an antibacterial peptide from hemocyanin of the freshwater crayfish *Pacifastacus leniusculus*, J. Biol. Chem. 278 (2003) 7927–7933.
[26] Y. Zhang, Y. Ma, M. Yang, S. Min, J. Yao, L. Zhu, Expression, purification, and refolding of a recombinant human bone morphogenetic protein 2 in vitro, Protein Expr. Purif. 75 (2011) 155–160.
[27] S.G. Kini, P.Q.T. Nguyen, S. Weissbach, A. Mallagaray, J. Shin, H.S. Yoon, Studies on the chitin-binding property of novel cysteine-rich peptides from Alternanthera sessilis, Biochemistry 54 (2015) 6639–6649.
[28] C.L. Wilson, A.J. Ouellette, D.P. Satchell, T. Ayabe, Y.S. Lo´pez-Boado, J.L. Stratman, S.J. Hultgren, L.M. Matrisian, W.C. Parks, Regulation of intestinal alpha-defensin activation by the metalloproteinase matrilysin in innate host defense, Science 286 (1999) 113–117.
[29] D. Ghosh, E. Porter, B. Shen, S.K. Lee, D. Wilk, J. Drazba, S.P. Yadav, J.W. Crabb, T. Ganz, C.L. Bevins, Paneth cell trypsin is the processing enzyme for human defensin-5, Nat. Immunol. 3 (2002) 583–590.
[30] H.H. Chuang, H.Y. Lin, F.P. Lin, Biochemical characteristics of c-terminal region of recombinant chitinase from bacillus licheniformis: implication of necessity for enzyme properties, FEBS J. 275 (2008) 2240–2254.
[31] T. Uchiyama, F. Katouno, N. Nikaidou, T. Nonaka, J. Sugiyama, T. Watanabe, Roles of the exposed aromatic residues in crystalline chitin hydrolysis by chitinase a from serratia marcescens 2170, J. Biol. Chem. 276 (2001) 4134341349.
[32] T. Watanabe, Y. Ariga, U. Sato, T. Toratani, M. Hashimoto, N. Nikaidou, Aromatic residues within the substrate-binding cleft of bacillus circulans chitinase a1 are essential for hydrolysis of crystalline chitin, Biochem. J. 376 (2003) 237–244.
[33] F. Driss, A. Baanannou, S. Rouis, I. Masmoudi, N. Zouari, S. Jaoua, Effect of the

chitin binding domain deletion from bacillus thuringiensis subsp. kurstaki chitinase chi255 on its stability in escherichia coli, Mol. Biotechnol. 36 (2007) 232–237.
[34] W. Suginta, P. Sirimontree, N. Sritho, T. Ohnuma, T. Fukamizo, The chitin-binding domain of a gh-18 chitinase from vibrio harveyi is crucial for chitin-chitinase interactions, Int. J. Biol. Macromol. 3 (2016) 1111–1117.
[35] Y. Fan, S. Guo, X. Pei, Y. Zhang, Z. Luo, P. Yan, Effects of chitin binding domain on enzymatic properties and insecticidal activity of bombyx mori, chitinase, World J. Microbiol. Biotechnol. 27 (2011) 1551–1558.
[36] S. Tantimavanich, S. Pantuwatana, A. Bhumiratana, W. Panbangred, Multiple chitinase enzymes from a single gene of bacillus licheniformis, tp-1, J. Ferment. Bioeng. 85 (1998) 259–265.
[37] H. Tsujibo, H. Orikoshi, H. Tanno, K. Fujimoto, K. Miyamoto, C. Imada, Cloning, sequence, and expression of a chitinase gene from a marine bacterium, altermonas sp. strain o-7, J. Bacteriol. 175 (1993) 176–181.
[38] H. Blaak, H. Schrempf, Binding and substrate specificities of a Streptomyces olivaceoviridis chitinase in comparison with its proteolytically processed form, FEBS J. 229 (2010) 132–139.
[39] A. Romaguera, U. Menge, R. Breves, H. Diekmann, Chitinases of Streptomyces olivaceoviridis and significance of processing for multiplicity, J. Bacteriol. 174 (1992) 3450–4345.
[40] M.J. Kuranda, P.W. Robbins, Chitinase is required for cell separation during growth of saccharomyces cerevisiae, J. Biol. Chem. 266 (1991) 19758–19767.
[41] S. Itoi, Y. Kanomata, Y. Koyama, K. Kadokura, S. Uchida, T. Nishio, Identification of a novel endochitinase from a marine bacterium vibrio proteolyticus strain no. 442, Biochim. Biophys. Acta 1774 (2007) 1099–1107.